

# Towards Learning of Filter-Level Heterogeneous Compression of Convolutional Neural Networks

**Yochai Zur \***

**Chaim Baskin \***

**Evgenii Zheltonozhskii**

**Brian Chmiel**

**Itay Evron**

**Alex M. Bronstein**

**Avi Mendelson**

*Department of Computer Science, Technion, Haifa, Israel*

YOCHAIZ@CS.TECHNION.AC.IL

CHAIMBASKIN@CS.TECHNION.AC.IL

EVGENIIZH@CAMPUS.TECHNION.AC.IL

BRIANCH@CAMPUS.TECHNION.AC.IL

EVRON.ITAY@GMAIL.COM

BRON@CS.TECHNION.AC.IL

AVI.MENDELSON@TCE.TECHNION.AC.IL

## Abstract

Recently, deep learning has become a *de facto* standard in machine learning with convolutional neural networks (CNNs) demonstrating spectacular success on a wide variety of tasks. However, CNNs are typically very demanding computationally at inference time. One of the ways to alleviate this burden on certain hardware platforms is *quantization* relying on the use of low-precision arithmetic representation for the weights and the activations. Another popular method is the pruning of the number of filters in each layer. While mainstream deep learning methods train the neural networks weights while keeping the network architecture fixed, the emerging neural architecture search (NAS) techniques make the latter also amenable to training. In this paper, we formulate optimal arithmetic bit length allocation and neural network pruning as a NAS problem, searching for the configurations satisfying a computational complexity budget while maximizing the accuracy. We use a differentiable search method based on the continuous relaxation of the search space proposed by Liu et al. (2019a). We show, by grid search, that heterogeneous quantized networks suffer from a high variance which renders the benefit of the search questionable. For pruning, improvement over homogeneous cases is possible, but it is still challenging to find those configurations with the proposed method. The code is publicly available at <https://github.com/yochaiz/Slimmable> and <https://github.com/yochaiz/darts-UNIQ>.

## 1. Introduction

Convolutional neural networks (CNNs) have become a main solution for computer vision tasks. However, high computation requirements complicate their usage in low-power systems. Recently, the machine learning approaches outperformed humans in design of CNNs (Zoph et al., 2018; Real et al., 2018; Macko et al., 2019; Ghiasi et al., 2019) and allowed to optimize complexity (Cai et al., 2019; Guo et al., 2019) or runtime (Tan et al., 2018; Chu et al., 2019;

---

\*. equal contributors

Stamoulis et al., 2019). Moreover, using gradient-based methods (Liu et al., 2019a; Noy et al., 2019) reduces search time to a couple of GPU-days.

We focus on two aspects of complexity reduction: quantization and pruning. Some recent works demonstrated that using 16– or even 8–bit representations do not harm accuracy of NNs (Gupta et al., 2015; Jacob et al., 2018; Lee et al., 2018). To reduce both runtime and power consumption, researches investigated further reduction of bitwidth, up to a single bit (Hubara et al., 2016; Bethge et al., 2018; Ding et al., 2019), which is impossible with naive techniques.

Alternatively, one could use fewer convolutional filters by proportionally reducing their number (Sandler et al., 2018) or by pruning insignificant ones (LeCun et al., 1990; Li et al., 2017). Recently, slimmable networks (Yu et al., 2019) offered a method to simultaneously train multiple instances of a CNN with different filter count.

Both methods compress the network with some parameter  $\alpha$  representing the bitwidth or the percentage of filters pruned. *Homogeneous* configurations use same value of  $\alpha$  along the network, *e.g.*, same bitwidth of parameters in each layer. Many quantization works employ simple *heterogeneous* configurations with different bitwidth in first or last layer (Zhou et al., 2016; Zhang et al., 2018; Hoffer et al., 2018; McKinstry et al., 2018; Choi et al., 2018). Some works studied a *layer-wise quantization granularity* (Louizos et al., 2017; Lacey et al., 2018). Heterogeneous configurations are often found in pruning too.

Recent works studied quantization with filter-wise quantization granularity (Wu et al., 2018; Yazdanbakhsh et al., 2018; Chen et al., 2018; Lou et al., 2019; Guo et al., 2019) and pruning (Liu et al., 2019b; Yu and Huang, 2019a) using NAS techniques. In this paper we study the opportunities of compression of the network with *filter-wise granularity*.

**Contribution** The main contribution of this paper are follows: study of variance of compressed networks; arithmetic compression on filter level; application of differentiable NAS to those problems.

The rest of the paper is organized as following: Section 2 introduces a general method, Sections 3 and 4 describe experiments performed, and Section 5 concludes the paper.

## 2. Method

**Differentiable search method** For CNN with  $L$  convolutional layers with  $C_\ell$  filters in layer  $\ell = 1, \dots, L$ , let  $T_\ell$  denote the set of compression operations that can be applied to one filter. Our goal is to find an optimal assignment of the said operations to each filter.

To do that, we aim to learn a probability of each operation to be chosen, similarly to Liu et al. (2019a). Referring to the operations in  $T_\ell$  simply by their index,  $i = 1, \dots, |T_\ell|$ , we assign to each operation  $i$  in layer  $\ell$  a parameter  $\alpha_{\ell i}$ , and denote by  $\hat{\alpha}_{\ell i} = f(\alpha_{\ell i})$  the probability to choose this particular operation. We also denote by  $\boldsymbol{\alpha}_\ell = (\alpha_{\ell 1}, \dots, \alpha_{\ell |T_\ell|})^T$  the vector of parameters in a given layer  $\ell$ , and by the pseudomatrix  $\boldsymbol{\alpha} = (\boldsymbol{\alpha}_1, \dots, \boldsymbol{\alpha}_L)$  the corresponding parameters of the entire network.

To reduce the search space size, instead of assigning operations to each filter independently we do it on layer level. Let  $a_{\ell i}$  denote the number of filters in the layer  $\ell$  to which the operation  $i$  is applied. We refer to the vector  $\mathbf{a}_\ell = (a_{\ell 1}, \dots, a_{\ell |T_\ell|})^\top$  with the elements summing to  $C_\ell$  defining the choice of the operations in layer  $\ell$  as to the *configuration* of the layer. We denote the configuration of the entire network by the pseudo-matrix  $\mathbf{a}$ .

Let  $\mathbf{A}_\ell$  be a random vector sampling which yields a specific configuration  $\mathbf{a}_\ell$  for layer  $\ell$ . The probability of the network configuration  $\mathbf{a}$  is given by

$$p(\mathbf{a}|\boldsymbol{\alpha}) = \prod_{\ell=1}^L \Pr(\mathbf{A}_\ell = \mathbf{a}_\ell). \quad (1)$$

Note that the latter probability depends on the  $\hat{\alpha}_\ell$ 's, which, in turn, depend on the  $\boldsymbol{\alpha}_\ell$ 's. The neural network is thus fully defined by the configuration  $\mathbf{a}$  and the weights  $\boldsymbol{\omega}$ .

Let  $\mathcal{L}(\mathbf{a}; \boldsymbol{\omega})$  denote the loss of the particular configuration  $\mathbf{a}$  with the weights  $\boldsymbol{\omega}$ . The expected loss over all network configurations with the same weights is given by

$$J(\boldsymbol{\alpha}; \boldsymbol{\omega}) = \mathbb{E}_{\boldsymbol{\alpha}} \mathcal{L}(\mathbf{a}; \boldsymbol{\omega}) = \sum_{\mathbf{a}} p(\mathbf{a}|\boldsymbol{\alpha}) \mathcal{L}(\mathbf{a}; \boldsymbol{\omega}), \quad (2)$$

where the sum is taken over all possible configurations. The goal of the search is to minimize the latter loss over  $\boldsymbol{\alpha}$  and  $\boldsymbol{\omega}$ , which is carried out using gradient steps.

Note that compared to the regular neural network training (optimization over  $\boldsymbol{\omega}$  with a single configuration), the number of additional optimization variables ( $\boldsymbol{\alpha}$ ) remains relatively modest. In sharp contrast, the number of configurations required to compute  $J$  is exponentially large, as shown in Lemmas 4 and 8 in the Appendix. For this reason, we approximate the gradient  $\mathbf{g} = \nabla_{\boldsymbol{\alpha}} J$  by sampling a subset  $S$  of possible configurations:

$$g_{\alpha_{\ell i}} \approx \hat{g}_{\alpha_{\ell i}} = \frac{1}{|S|} \sum_{\mathbf{a} \in S} \mathcal{L}(\mathbf{a}; \boldsymbol{\omega}) \cdot (a_{\ell i} - C_\ell \cdot \hat{\alpha}_{\ell i}). \quad (3)$$

The sample size  $|S|$  governs the tradeoff between the complexity of the training and the estimator variance. The gradient with respect to the weights  $\boldsymbol{\omega}$  is computed as usual.

**Loss** We use bit operations (BOPs) (Baskin et al., 2018b) as a complexity metric in the case of quantization. BOPs refers to the number of bit operations needed to perform inference. Since the bitwidth of operands might be different, we extend the definition of Baskin et al. (2018b) to this case. The exact derivation of the BOPs metric is provided Appendix F. Neither FLOPs nor BOPs predict the runtime of the network (Tan et al., 2018; Cai et al., 2019; Li et al., 2019), but can still be used as a proxy to the performance.

Let us denote the complexity of layer  $\ell$  by  $\mathcal{B}_\ell(\mathbf{a})$ ; the metric is defined in Eq. (31) in the Appendix for the quantized CNN case, and simply equals to the MAC count of the layer in all other cases. We define the computational complexity loss as

$$\mathcal{L}_{\text{com}}(\mathbf{a}) \triangleq \sigma \left( \sum_{\ell=1}^L \mathcal{B}_\ell(\mathbf{a}) \right), \quad (4)$$

where  $\sigma$  is some increasing function. Note that  $\mathcal{L}_{\text{com}}(\mathbf{a})$  only depends on the network configuration and penalizes configurations  $\mathbf{a}$  with high complexity. In particular,  $\sigma$  can be a function of the ratio between  $\mathbf{a}$  arithmetic complexity and the complexity of some target homogeneous configuration, which allows to set a target complexity for the search.

The combined loss  $\mathcal{L}(\mathbf{a}; \boldsymbol{\omega})$  appearing in (3) is a linear combination of the standard loss used to train the network w.r.t. the weights,  $\mathcal{L}_{\text{acc}}(\mathbf{a}; \boldsymbol{\omega})$ , and the complexity loss,

$$\mathcal{L}(\mathbf{a}; \boldsymbol{\omega}) = \mathcal{L}_{\text{acc}}(\mathbf{a}; \boldsymbol{\omega}) + \lambda \cdot \mathcal{L}_{\text{com}}(\mathbf{a}), \quad (5)$$

embodying the tradeoff between the network accuracy and complexity.

### 3. Quantized NAS

Quantization was one of the evaluated compression methods. We used ResNet-20 (He et al., 2016) on CIFAR-10 (Krizhevsky, 2009). The network was quantized with NICE (Baskin et al., 2018a), with the operations set  $T_\ell$  consisting of tuples  $(b_w, b_a)$  of weight and output activation bitwidths, respectively.  $\mathbf{A}_\ell \sim \text{Multinomial}(C_\ell, (\hat{\alpha}_{\ell 1}, \hat{\alpha}_{\ell 2}, \dots, \hat{\alpha}_{\ell |T_\ell|}))$  is multinomial random variable, with the probabilities  $\hat{\alpha}_\ell$  obtained from  $\boldsymbol{\alpha}$  using softmax.

Sampling a layer configuration  $a_\ell = (a_{\ell 1}, \dots, a_{\ell |T_\ell|})$  induces a specific structure over the filters, shown in Fig. A.1 in the Appendix. For  $T_\ell = \{t_1, t_2, \dots, t_{|T_\ell|}\}$ , we apply quantization with bitwidth tuple  $t_1$  on the first  $a_{\ell 1}$  filters,  $t_2$  on the next  $a_{\ell 2}$  filters and so on.

In our experiments, we selected the set  $T_\ell = \{(2, 2), (2, 4), (3, 3), (8, 8)\}$  for all the layers. A few configurations were trained multiple times under the same conditions. We conclude that though the search yields well-performing configurations (Fig. 2a and Appendix B.1.1), the variance of the accuracy is high, as shown in Fig. 1a. Thus, it is impossible to establish whether the configurations would be good in a different realization.

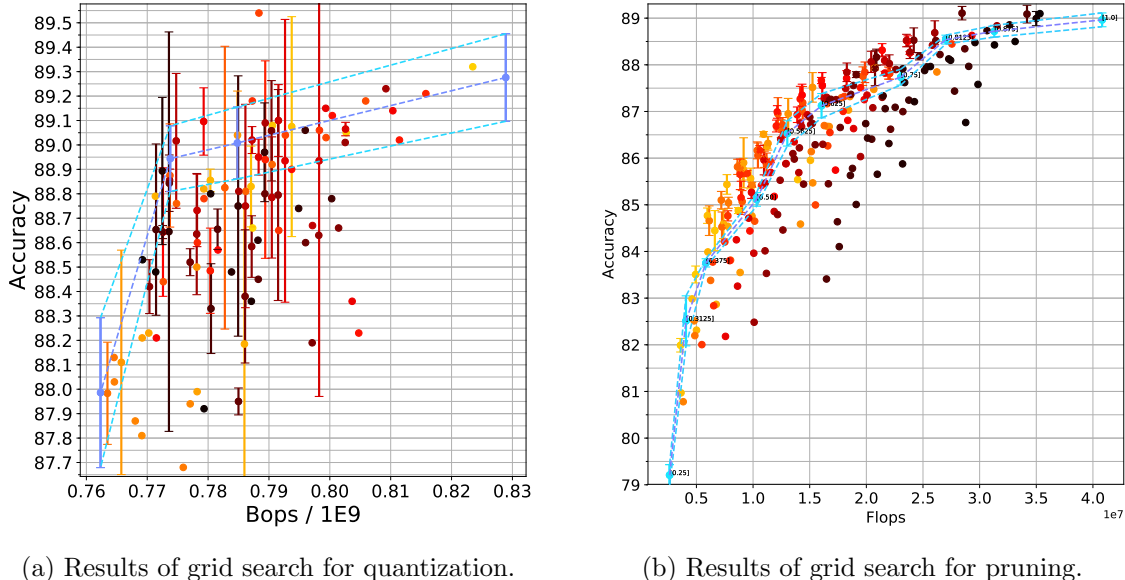
### 4. Slimmable NAS

Another compression method we considered is a reduction of number of filters in convolutional layers. In particular, we used slimmable networks framework (Yu et al., 2019; Yu and Huang, 2019b), in which networks with the same architecture but different amount of filters are trained simultaneously with the same weights. The operations set  $T_\ell = \{1, \dots, C_\ell\}$  represents the number of filters in a layer  $\ell$ . We set  $\mathbf{A}_\ell \sim \text{Binomial}(C_\ell - 1, \hat{\alpha}_\ell)$  as binomial a random variable, and use a sigmoid normalization of the distribution parameters,

$$\hat{\alpha}_\ell = \frac{\exp\{\alpha_\ell\}}{\exp\{\alpha_\ell\} + 1} \quad (6)$$

Sampling a configuration from  $\mathbf{A}_\ell$  determines the number of filters in the layer.

Similarly to Section 3, we explored the search space by evaluating ResNet-20 configurations with setup described in Appendix A.1. As shown in Fig. 1b, the variance is relatively low, though it is still higher for heterogeneous configurations. Points with statistically significant improvement over homogeneous configuration were also found.



(a) Results of grid search for quantization.

(b) Results of grid search for pruning.

Figure 1: Results of grid search in both cases. Blue line connects homogeneous configurations, colored points are heterogeneous configurations. Error bars are for 0.6827 confidence interval. More details in Figs. B.1 and B.2.

**Basic search method** At each iteration, we sample a set of configurations  $S_k$  from current distribution  $\hat{\alpha}^k$  for gradient estimation. To improve the loss evaluation we duplicate the current network weights and fine-tune each configuration  $a \in S_k$  for 5 epochs.

We define the expected configuration  $\mathcal{A}^{\hat{\alpha}}$  such that  $\mathcal{A}_l^{\hat{\alpha}} = \text{round}(\mathbb{E}[\mathcal{A}_l])$ . The network weights are trained over 5 configurations: 4 homogeneous ones ( $\{0.25, 0.5, 0.75, 1.0\}$ ) and one defined by  $\mathcal{A}^{\hat{\alpha}}$ . Since samples from  $\hat{\alpha}^k$  would be close to the expectation of their distribution,  $\omega$  should be a better starting point to train the sampled configurations.

**Resetting the  $\omega$**  We noticed that after few iterations of the network weights updates on  $A \cup \mathcal{A}^{\hat{\alpha}^k}$ , the validation loss of  $\mathcal{A}^{\hat{\alpha}^k}$  was high compared to the homogeneous configurations in  $A$ . We conjectured that the network overfits to the homogeneous configurations which are kept same while  $\mathcal{A}^{\hat{\alpha}^k}$  changes. To avoid the overfitting, we reinitialize  $\omega$  after each iteration. Additional changes, detailed in Appendix C.3, were done.

**Disabling weight-sharing** In addition, the overly short fine-tuning leads to inaccurate configuration evaluation. Thus instead of sharing and fine-tuning  $\omega$  we trained each configuration  $a$ , individually, with individual weights set  $\omega_{1,2,\dots,L}$ , from scratch.

**Interpolation loss** To achieve the goal of improvement over homogeneous configurations, we tried to compare the heterogeneous configuration cross-entropy with the expected one, by defining the loss as a difference from interpolation of known homogeneous configurations (details in Appendix C.5). The results are shown on Fig. 2b and in Appendix B.1.2.

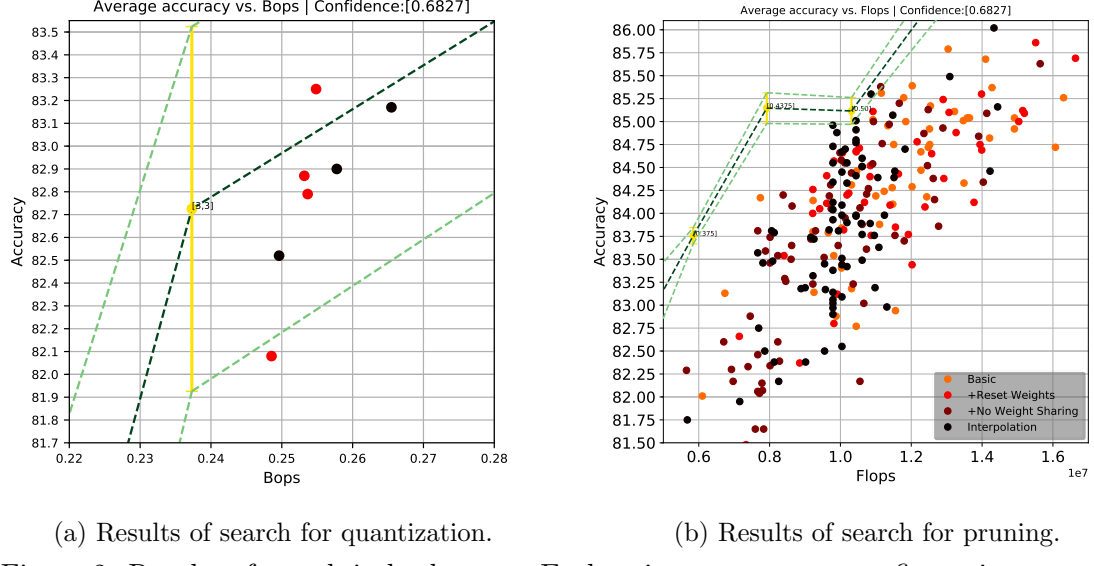


Figure 2: Results of search in both cases. Each point represents a configuration proposed by search. More details in Appendix B.1.

## 5. Conclusion

In this paper, we studied the feasibility of using NAS-like algorithms, and in particular differentiable NAS (Liu et al., 2019a), for the reduction of CNN complexity by means of filter-wise quantization and layer-wise pruning. In both cases, we applied our method for ResNet-20 on CIFAR-10, on which it took only 36 GPU-hours to converge.

For filter-wise quantization, after acquiring nominal improvement over the homogeneous baseline, we found out that the variance of heterogeneous configurations is too high to warrant a significant improvement, which we confirmed using partial grid search. Unfortunately, previous studies on bitwidth allocation or architecture-quantization search (Wu et al., 2018; Yazdanbakhsh et al., 2018; Chen et al., 2018; Lou et al., 2019; Guo et al., 2019) did not report the variance of the results, making meaningful comparison impossible. For layer-wise pruning, we obtained more stable results, with the grid search confirming the possibility of improvement over the baseline homogeneous configurations. However, the heterogeneous configurations found by NAS did not significantly outperform the baseline.

We conclude that future work should focus on loss design and better loss estimators, such as Gumbel softmax (Jang et al., 2017). Successfully transferring the architecture to a more challenging use case (*e.g.*, ImageNet) remains another important challenge.

## Acknowledgments

The research was funded by Hyundai Motor Company through HYUNDAI-TECHNION-KAIST Consortium, ERC StG RAPID and Hiroshi Fujiwara Technion Cyber Security Research Center.

## References

- Chaim Baskin, Natan Liss, Yoav Chai, Evgenii Zheltonozhskii, Eli Schwartz, Raja Girayes, Avi Mendelson, and Alexander M Bronstein. Nice: Noise injection and clamping estimation for neural network quantization. *arXiv preprint arXiv:1810.00162*, 2018a. URL <https://arxiv.org/abs/1810.00162>. (cited on p. 4)
- Chaim Baskin, Eli Schwartz, Evgenii Zheltonozhskii, Natan Liss, Raja Girayes, Alex M Bronstein, and Avi Mendelson. Uniq: Uniform noise injection for non-uniform quantization of neural networks. *arXiv preprint arXiv:1804.10969*, 2018b. URL <https://arxiv.org/abs/1804.10969>. (cited on pp. 3 and 33)
- Joseph Bethge, Marvin Bornstein, Adrian Loy, Haojin Yang, and Christoph Meinel. Training competitive binary neural networks from scratch. *arXiv preprint arXiv:1812.01965*, 2018. URL <https://arxiv.org/abs/1812.01965>. (cited on p. 2)
- Han Cai, Ligeng Zhu, and Song Han. ProxylessNAS: Direct neural architecture search on target task and hardware. In *International Conference on Learning Representations*, 2019. URL <https://openreview.net/forum?id=HylVB3AqYm>. (cited on pp. 1 and 3)
- Yukang Chen, Gaofeng Meng, Qian Zhang, Xinbang Zhang, Liangchen Song, Shiming Xiang, and Chunhong Pan. Joint neural architecture search and quantization. *arXiv preprint arXiv:1811.09426*, 2018. URL <https://arxiv.org/abs/1811.09426>. (cited on pp. 2 and 6)
- Jungwook Choi, Pierce I-Jen Chuang, Zhuo Wang, Swagath Venkataramani, Vijayalakshmi Srinivasan, and Kailash Gopalakrishnan. Bridging the accuracy gap for 2-bit quantized neural networks (qnn). *arXiv preprint arXiv:1807.06964*, 2018. URL <https://arxiv.org/abs/1807.06964>. (cited on p. 2)
- Xiangxiang Chu, Bo Zhang, Ruijun Xu, and Hailong Ma. Multi-objective reinforced evolution in mobile neural architecture search. *arXiv preprint arXiv:1901.01074*, 2019. URL <https://arxiv.org/abs/1901.01074>. (cited on p. 1)
- Ruizhou Ding, Ting-Wu Chin, Zeye Liu, and Diana Marculescu. Regularizing activation distribution for training binarized deep networks. *arXiv preprint arXiv:1904.02823*, 2019. URL <https://arxiv.org/abs/1904.02823>. (cited on p. 2)
- Golnaz Ghiasi, Tsung-Yi Lin, Ruoming Pang, and Quoc V. Le. NAS-FPN: Learning Scalable Feature Pyramid Architecture for Object Detection. *arXiv preprint arXiv:1904.07392*, 2019. URL <https://arxiv.org/abs/1904.07392>. (cited on p. 1)
- Zichao Guo, Xiangyu Zhang, Haoyuan Mu, Wen Heng, Zechun Liu, Yichen Wei, and Jian Sun. Single Path One-Shot Neural Architecture Search with Uniform Sampling. *arXiv*

*preprint arXiv:1904.00420*, 2019. URL <https://arxiv.org/abs/1904.00420>. (cited on pp. 1, 2, and 6)

Suyog Gupta, Ankur Agrawal, Kailash Gopalakrishnan, and Pritish Narayanan. Deep learning with limited numerical precision. In Francis Bach and David Blei, editors, *Proceedings of the 32nd International Conference on Machine Learning*, volume 37 of *Proceedings of Machine Learning Research*, pages 1737–1746, Lille, France, 07–09 Jul 2015. PMLR. URL <http://proceedings.mlr.press/v37/gupta15.html>. (cited on p. 2)

Kaiming He, Xiangyu Zhang, Shaoqing Ren, and Jian Sun. Deep residual learning for image recognition. In *The IEEE Conference on Computer Vision and Pattern Recognition (CVPR)*, June 2016. URL [http://openaccess.thecvf.com/content\\_cvpr\\_2016/html/He\\_Deep\\_Residual\\_Learning\\_CVPR\\_2016\\_paper.html](http://openaccess.thecvf.com/content_cvpr_2016/html/He_Deep_Residual_Learning_CVPR_2016_paper.html). (cited on pp. 4 and 13)

Elad Hoffer, Itay Hubara, and Daniel Soudry. Fix your classifier: the marginal value of training the last weight layer. In *International Conference on Learning Representations*, 2018. URL <https://openreview.net/forum?id=S1Dh8Tg0->. (cited on p. 2)

Itay Hubara, Matthieu Courbariaux, Daniel Soudry, Ran El-Yaniv, and Yoshua Bengio. Binarized neural networks. In D. D. Lee, M. Sugiyama, U. V. Luxburg, I. Guyon, and R. Garnett, editors, *Advances in Neural Information Processing Systems 29*, pages 4107–4115. Curran Associates, Inc., 2016. URL <http://papers.nips.cc/paper/6573-binarized-neural-networks.pdf>. (cited on p. 2)

Benoit Jacob, Skirmantas Kligys, Bo Chen, Menglong Zhu, Matthew Tang, Andrew Howard, Hartwig Adam, and Dmitry Kalenichenko. Quantization and training of neural networks for efficient integer-arithmetic-only inference. In *The IEEE Conference on Computer Vision and Pattern Recognition (CVPR)*, June 2018. URL [http://openaccess.thecvf.com/content\\_cvpr\\_2018/html/Jacob\\_Quantization\\_and\\_Training\\_CVPR\\_2018\\_paper.html](http://openaccess.thecvf.com/content_cvpr_2018/html/Jacob_Quantization_and_Training_CVPR_2018_paper.html). (cited on p. 2)

Eric Jang, Shixiang Gu, and Ben Poole. Categorical reparameterization with gumbel-softmax. In *International Conference on Learning Representations*, 2017. URL <https://openreview.net/forum?id=rkE3y85ee>. (cited on p. 6)

William Kahan. Ieee standard 754 for binary floating-point arithmetic. *Lecture Notes on the Status of IEEE*, 754(94720-1776):11, 1996. URL <https://people.eecs.berkeley.edu/~wkahan/ieee754status/IEEE754.PDF>. (cited on p. 33)

Alex Krizhevsky. Learning multiple layers of features from tiny images. Master’s thesis, Department of Computer Science, University of Toronto, 2009. URL <http://citeseerx.ist.psu.edu/viewdoc/summary?doi=10.1.1.222.9220>. (cited on p. 4)

- Griffin Lacey, Graham W. Taylor, and Shawki Areibi. Stochastic layer-wise precision in deep neural networks. In *Proceedings of the 34th Annual Conference on Uncertainty in Artificial Intelligence (UAI-18)*, 2018. URL <https://arxiv.org/abs/1807.00942>. (cited on p. 2)
- Yann LeCun, John S. Denker, and Sara A. Solla. Optimal brain damage. In D. S. Touretzky, editor, *Advances in Neural Information Processing Systems 2*, pages 598–605. Morgan-Kaufmann, 1990. URL <http://papers.nips.cc/paper/250-optimal-brain-damage.pdf>. (cited on p. 2)
- Jun Haeng Lee, Sangwon Ha, Saerom Choi, Won-Jo Lee, and Seungwon Lee. Quantization for rapid deployment of deep neural networks. *arXiv preprint arXiv:1810.05488*, 2018. URL <https://arxiv.org/abs/1810.05488>. (cited on p. 2)
- Hao Li, Asim Kadav, Igor Durdanovic, Hanan Samet, and Hans Peter Graf. Pruning filters for efficient convnets. In *International Conference on Learning Representations*, 2017. URL <https://openreview.net/forum?id=rJqFGTslg>. (cited on p. 2)
- Xin Li, Yiming Zhou, Zheng Pan, and Jiashi Feng. Partial order pruning: for best speed/accuracy trade-off in neural architecture search. *arXiv preprint arXiv:1903.03777*, 2019. URL <https://arxiv.org/abs/1903.03777>. (cited on p. 3)
- Hanxiao Liu, Karen Simonyan, and Yiming Yang. DARTS: Differentiable architecture search. In *International Conference on Learning Representations*, 2019a. URL <https://openreview.net/forum?id=S1eYHoC5FX>. (cited on pp. 1, 2, and 6)
- Zechun Liu, Haoyuan Mu, Xiangyu Zhang, Zichao Guo, Xin Yang, Tim Kwang-Ting Cheng, and Jian Sun. Metapruning: Meta learning for automatic neural network channel pruning. *arXiv preprint arXiv:1903.10258*, 2019b. URL <https://arxiv.org/abs/1903.10258>. (cited on p. 2)
- Qian Lou, Lantao Liu, Minje Kim, and Lei Jiang. Autoqb: Automl for network quantization and binarization on mobile devices. *arXiv preprint arXiv:1902.05690*, 2019. URL <https://arxiv.org/abs/1902.05690>. (cited on pp. 2 and 6)
- Christos Louizos, Karen Ullrich, and Max Welling. Bayesian compression for deep learning. In I. Guyon, U. V. Luxburg, S. Bengio, H. Wallach, R. Fergus, S. Vishwanathan, and R. Garnett, editors, *Advances in Neural Information Processing Systems 30*, pages 3288–3298. Curran Associates, Inc., 2017. URL <http://papers.nips.cc/paper/6921-bayesian-compression-for-deep-learning.pdf>. (cited on p. 2)
- Vladimir Macko, Charles Weill, Hanna Mazzawi, and Javier Gonzalvo. Improving neural architecture search image classifiers via ensemble learning. *arXiv preprint arXiv:1903.06236*, 2019. URL <https://arxiv.org/abs/1903.06236>. (cited on p. 1)

Jeffrey L. McKinstry, Steven K Esser, Rathinakumar Appuswamy, Deepika Bablani, John V. Arthur, Izzet B Yildiz, and Dharmendra S. Modha. Discovering low-precision networks close to full-precision networks for efficient embedded inference. *arXiv preprint arXiv:1809.04191*, 2018. URL <https://arxiv.org/abs/1809.04191>. (cited on p. 2)

Asaf Noy, Niv Nayman, Tal Ridnik, Nadav Zamir, Sivan Doveh, Itamar Friedman, Raja Giryes, and Lihi Zelnik-Manor. ASAP: Architecture Search, Anneal and Prune. *arXiv preprint arXiv:1904.04123*, 2019. URL <https://arxiv.org/abs/1904.04123>. (cited on p. 2)

Esteban Real, Alok Aggarwal, Yanping Huang, and Quoc V. Le. Regularized evolution for image classifier architecture search. *arXiv preprint arXiv:1802.01548*, 2018. URL <https://arxiv.org/abs/1802.01548>. (cited on p. 1)

Mark Sandler, Andrew Howard, Menglong Zhu, Andrey Zhmoginov, and Liang-Chieh Chen. Mobilenetv2: Inverted residuals and linear bottlenecks. In *The IEEE Conference on Computer Vision and Pattern Recognition (CVPR)*, June 2018. URL [http://openaccess.thecvf.com/content\\_cvpr\\_2018/html/Sandler\\_MobileNetV2\\_Inverted\\_Residuals\\_CVPR\\_2018\\_paper.html](http://openaccess.thecvf.com/content_cvpr_2018/html/Sandler_MobileNetV2_Inverted_Residuals_CVPR_2018_paper.html). (cited on p. 2)

Dimitrios Stavroulis, Ruizhou Ding, Di Wang, Dimitrios Lymberopoulos, Bodhi Priyantha, Jie Liu, and Diana Marculescu. Single-Path NAS: Designing Hardware-Efficient ConvNets in less than 4 Hours. *arXiv preprint arXiv:1904.02877*, 2019. URL <https://arxiv.org/abs/1904.02877>. (cited on p. 2)

Mingxing Tan, Bo Chen, Ruoming Pang, Vijay Vasudevan, and Quoc V. Le. Mnasnet: Platform-aware neural architecture search for mobile. *arXiv preprint arXiv:1807.11626*, 2018. URL <https://arxiv.org/abs/1807.11626>. (cited on pp. 1 and 3)

Bichen Wu, Yanghan Wang, Peizhao Zhang, Yuandong Tian, Peter Vajda, and Kurt Keutzer. Mixed precision quantization of convnets via differentiable neural architecture search. *arXiv preprint arXiv:1812.00090*, 2018. URL <https://arxiv.org/abs/1812.00090>. (cited on pp. 2 and 6)

Amir Yazdanbakhsh, Ahmed T. Elthakeb, Prannoy Pilligundla, Fatemeh Sadat Mireshghalah, and Hadi Esmaeilzadeh. Releq: A reinforcement learning approach for deep quantization of neural networks. *arXiv preprint arXiv:1811.01704*, 2018. URL <https://arxiv.org/abs/1811.01704>. (cited on pp. 2 and 6)

Chris Ying, Aaron Klein, Esteban Real, Eric Christiansen, Kevin Murphy, and Frank Hutter. Nas-bench-101: Towards reproducible neural architecture search. *arXiv preprint arXiv:1902.09635*, 2019. URL <https://arxiv.org/abs/1902.09635>. (cited on p. 13)

- Jiahui Yu and Thomas Huang. Network slimming by slimmable networks: Towards one-shot architecture search for channel numbers. *arXiv preprint arXiv:1903.11728*, 2019a. URL <https://arxiv.org/abs/1903.11728>. (cited on p. 2)
- Jiahui Yu and Thomas Huang. Universally slimmable networks and improved training techniques. *arXiv preprint arXiv:1903.05134*, 2019b. URL <https://arxiv.org/abs/1903.05134>. (cited on p. 4)
- Jiahui Yu, Linjie Yang, Ning Xu, Jianchao Yang, and Thomas Huang. Slimmable neural networks. In *International Conference on Learning Representations*, 2019. URL <https://openreview.net/forum?id=H1gMCsAqY7>. (cited on pp. 2 and 4)
- Dongqing Zhang, Jiaolong Yang, Dongqiangzi Ye, and Gang Hua. Lq-nets: Learned quantization for highly accurate and compact deep neural networks. In *The European Conference on Computer Vision (ECCV)*, September 2018. URL [http://openaccess.thecvf.com/content\\_ECCV\\_2018/papers/Dongqing\\_Zhang\\_Optimized\\_Quantization\\_for\\_ECCV\\_2018\\_paper.pdf](http://openaccess.thecvf.com/content_ECCV_2018/papers/Dongqing_Zhang_Optimized_Quantization_for_ECCV_2018_paper.pdf). (cited on p. 2)
- Shuchang Zhou, Yuxin Wu, Zekun Ni, Xinyu Zhou, He Wen, and Yuheng Zou. Dorefa-net: Training low bitwidth convolutional neural networks with low bitwidth gradients. *arXiv preprint arXiv:1606.06160*, 2016. URL <https://arxiv.org/abs/1606.06160>. (cited on p. 2)
- Barret Zoph, Vijay Vasudevan, Jonathon Shlens, and Quoc V. Le. Learning transferable architectures for scalable image recognition. In *The IEEE Conference on Computer Vision and Pattern Recognition (CVPR)*, June 2018. URL [http://openaccess.thecvf.com/content\\_cvpr\\_2018/papers/Zoph\\_Learning\\_Transferable\\_Architectures\\_CVPR\\_2018\\_paper.pdf](http://openaccess.thecvf.com/content_cvpr_2018/papers/Zoph_Learning_Transferable_Architectures_CVPR_2018_paper.pdf). (cited on p. 1)

## Appendix A. Configurations

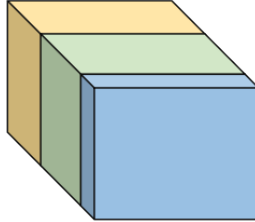


Figure A.1: Layer structure induced by sampling a configuration from a multinomial random variable. Assume  $T_\ell = \{t_1, t_2, t_3\}$ , we apply quantization with bitwidth  $t_1$  on the blue filters,  $t_2$  on the green filters and  $t_3$  on the yellow filters.

### A.1 Configuration of search space

Similarly to Ying et al. (2019), we performed a grid search on a simplified search space. ResNet-20 (He et al., 2016) was chosen as a basic architecture. This architecture has three blocks of convolutional layers, with increasing number of filters and decreasing dimensions of features. To reduce the required resources, the number of filters was reduced to 16, 32, and 64 in each group. For the quantization search space we sampled few layer configurations. Each sampled layer configuration, denote as  $a$ , induces a network configuration by setting each of the network layers configuration to  $a$ . We train each network configuration 3 times under the same conditions. The stopping criteria is 150 consecutive epochs without new optimal validation accuracy. For the pruning search space we sampled blocks configurations triplets. Each triplet induces a network configuration, where each layer in a specific block has the same layer configuration as any other layer in the specific block. As we did for the quantization search space, we train each network configuration 3 times under the same conditions. The stopping criteria is also the same.

### A.2 Transfer learning to ImageNet

We took 3 configurations with significant accuracy difference between them on CIFAR-10 and trained them on ImageNet. We found out that the configurations ranking on CIFAR-10 is different than their ranking on ImageNet, *i.e.*, a configuration might be optimal on CIFAR-10 but average on ImageNet.

## Appendix B. Additional results analysis

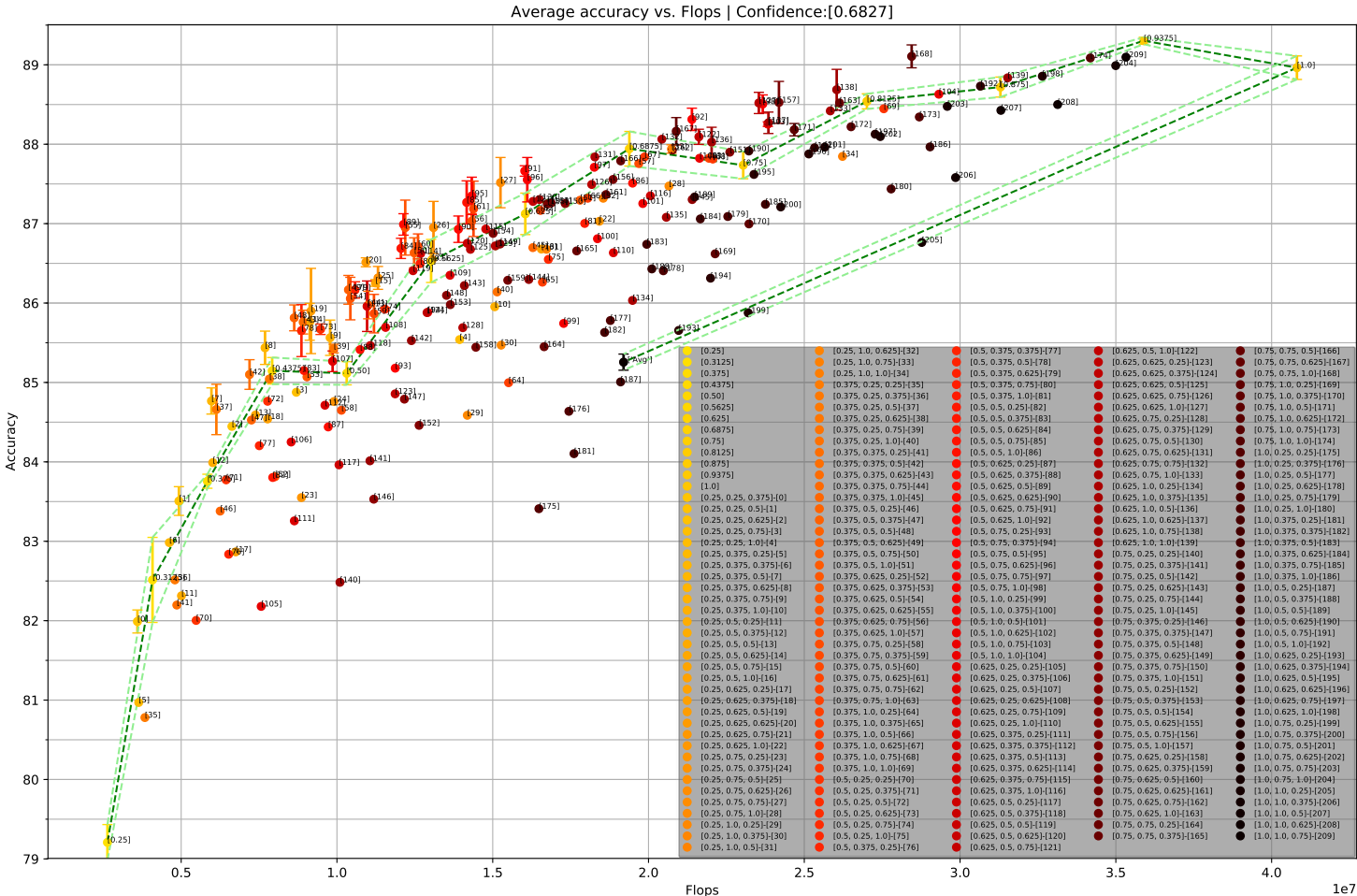
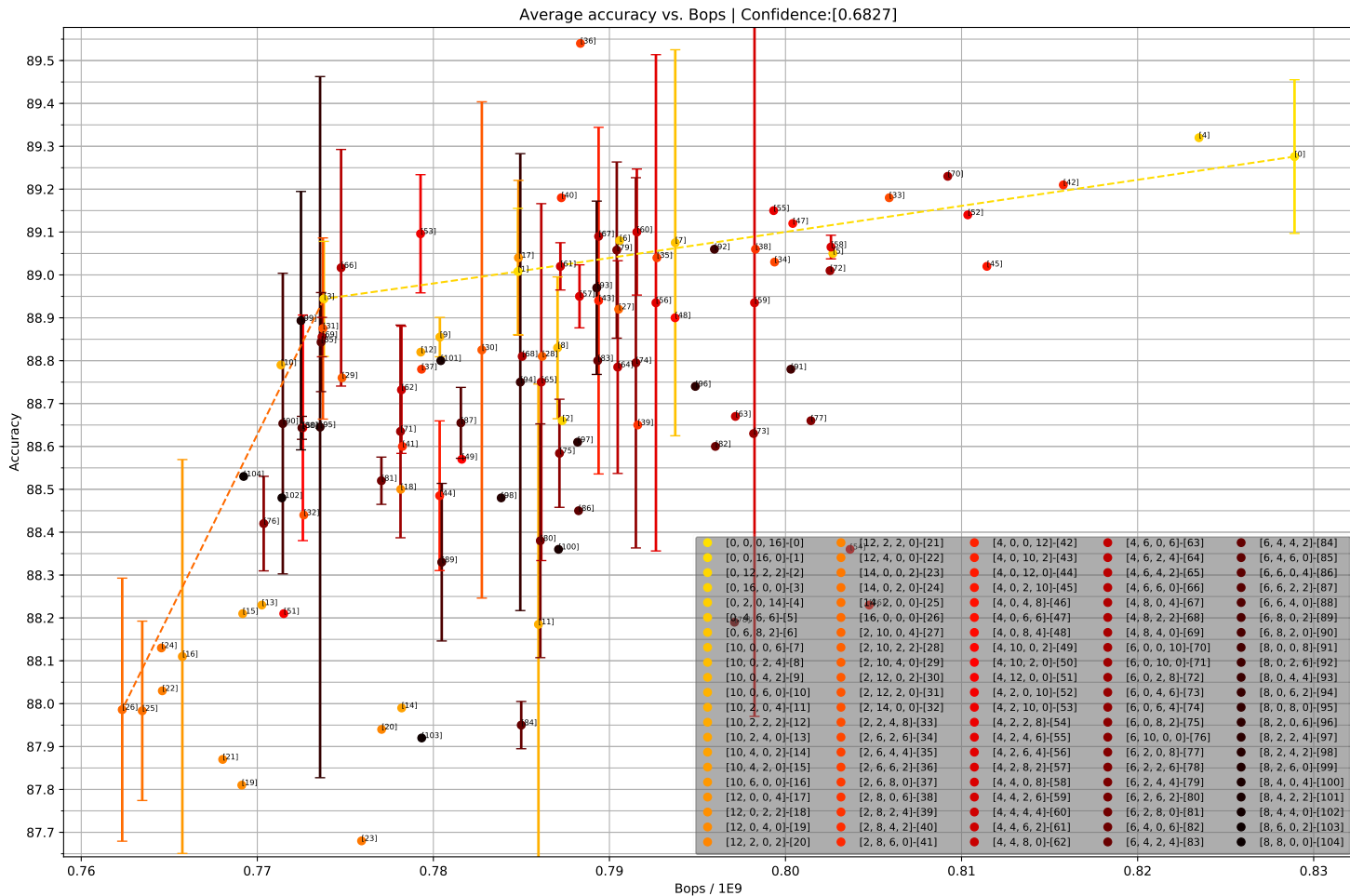
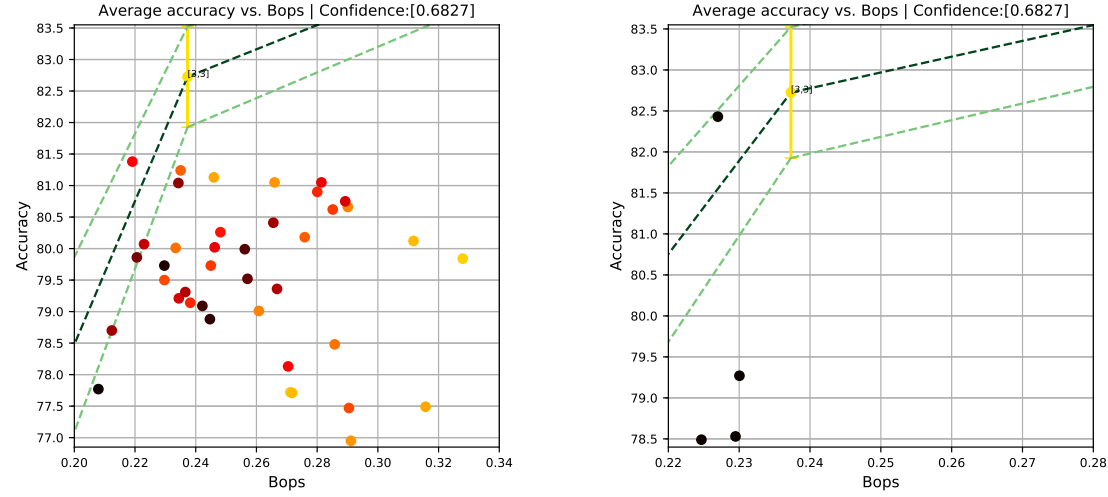


Figure B.1: Slimmable validation accuracy variance exploration plot. Each point represents a different configuration. The points connected in dashed line are the homogeneous configurations. The error bar represents 0.6827 confidence interval.



## B.1 Results

### B.1.1 QUANTIZATION



(a) Homogeneous configuration target is (3,3). (b) Homogeneous configuration target is (2,4).

Figure B.3: Additional results of search in quantization case.  $\lambda = 1$ .  $T_\ell = \{(2, 2), (2, 4), (3, 3), (8, 8)\}$

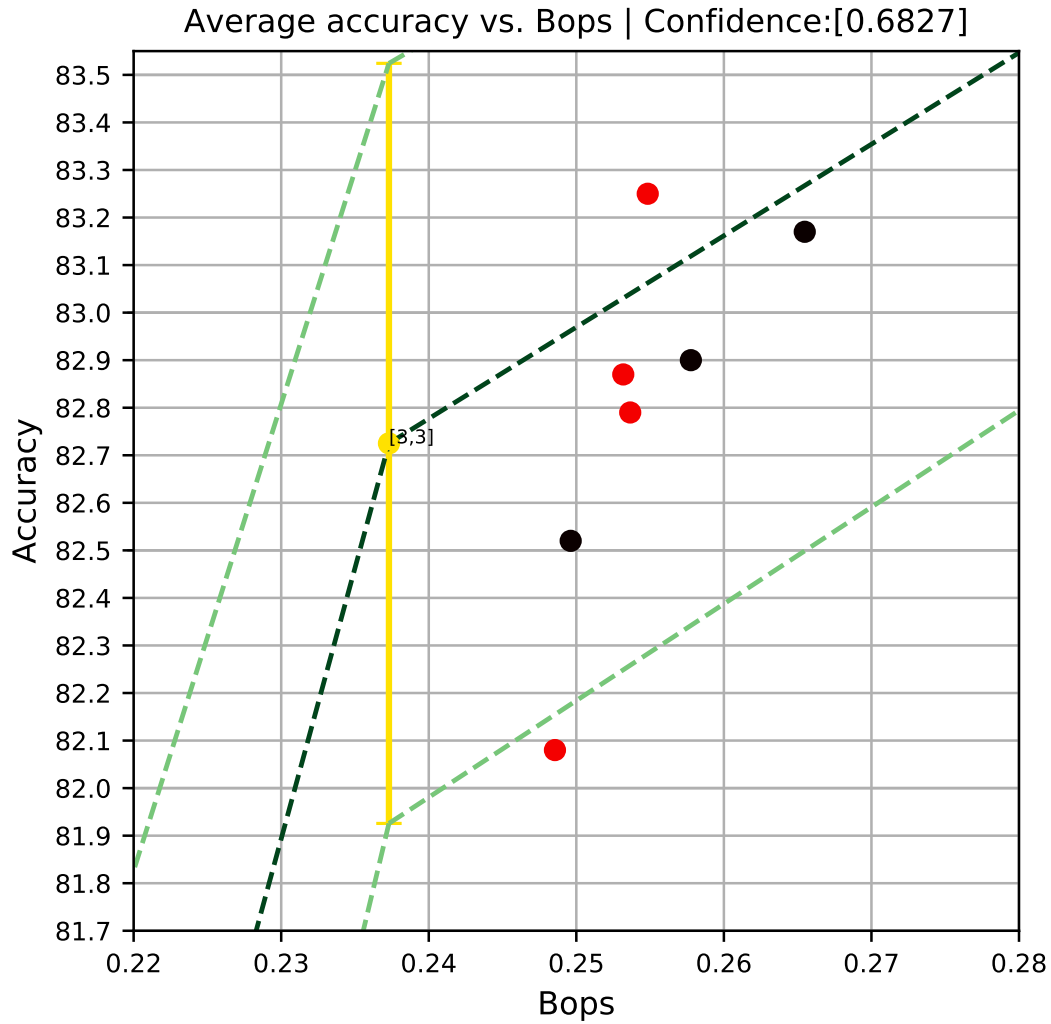


Figure B.4: Additional results of search in quantization case.  $\lambda = 1$ . Homogeneous configuration target is  $(3,3)$ .  $T_\ell = \{(2, 2), (3, 3), (4, 4), (8, 3), (8, 8)\}$ .

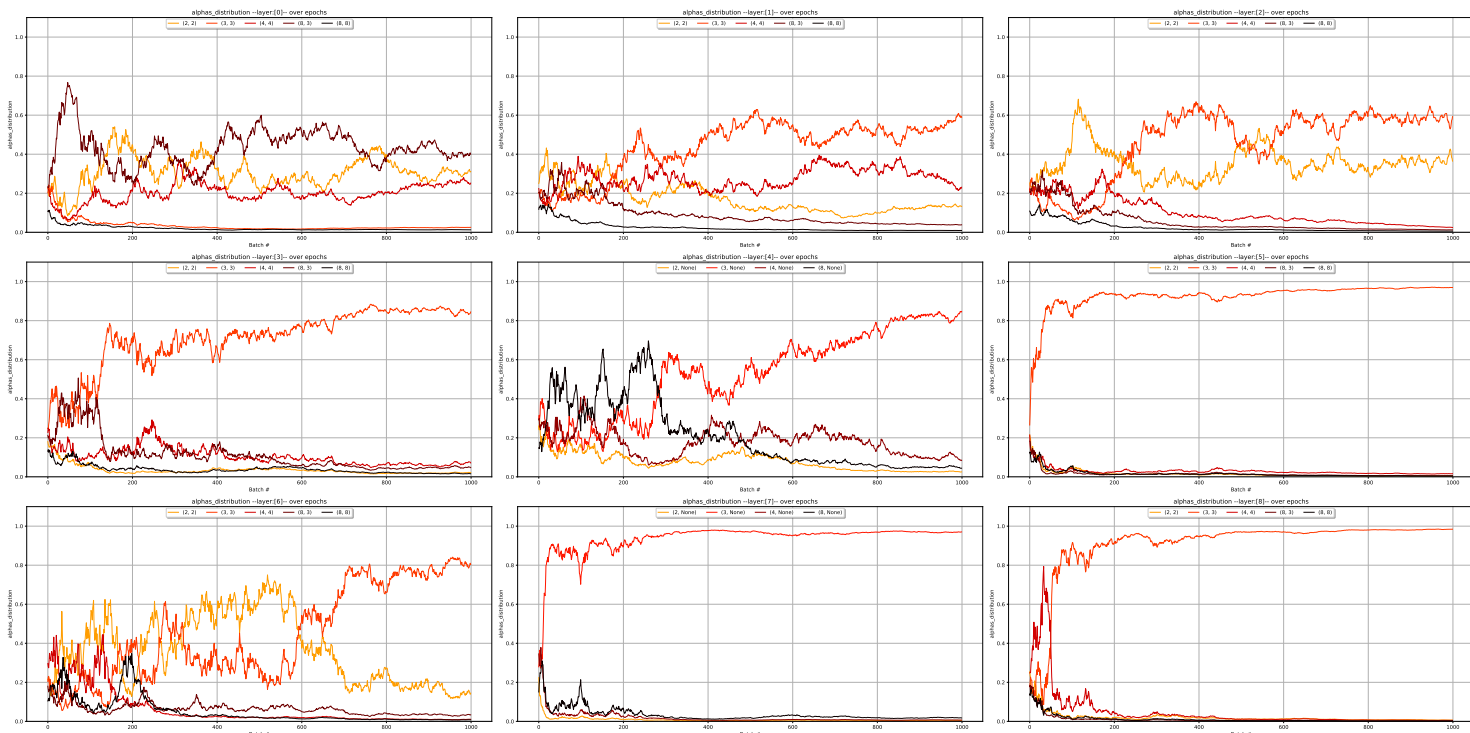
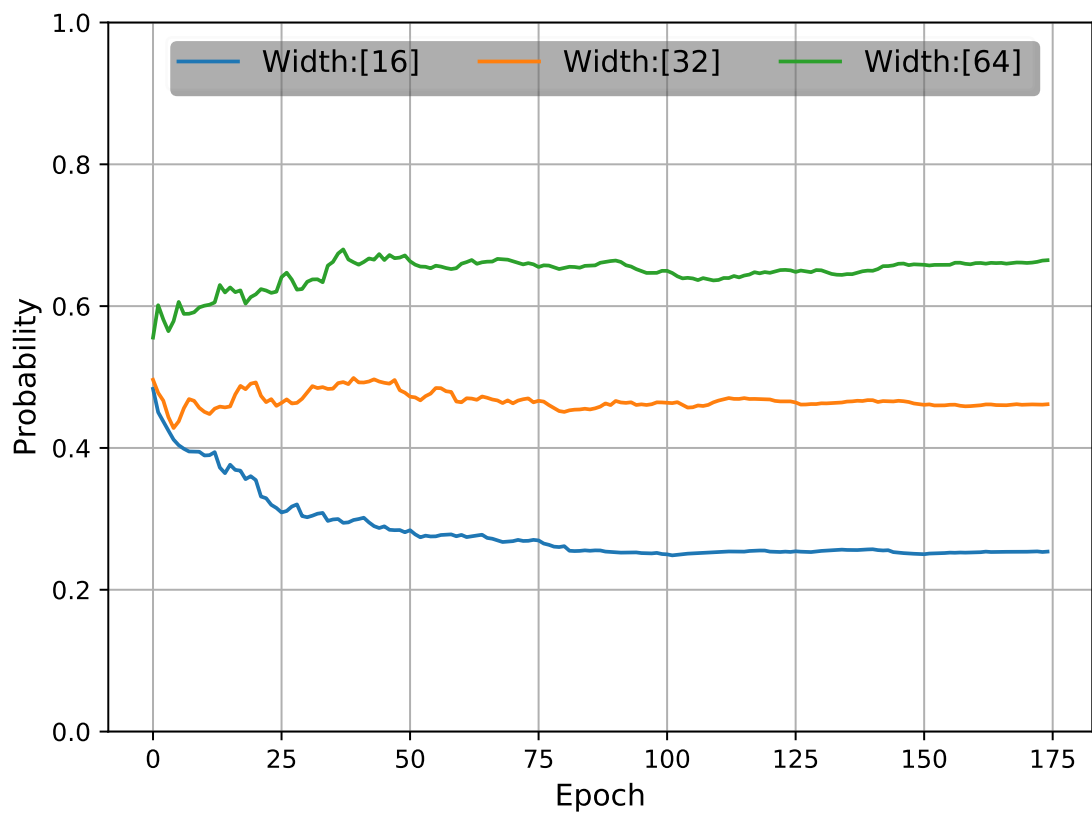


Figure B.5: Convergence of  $\alpha$  as a function of time in quantization case

## B.1.2 PRUNING

Figure B.6: Convergence of  $\alpha$  as a function of time in pruning case

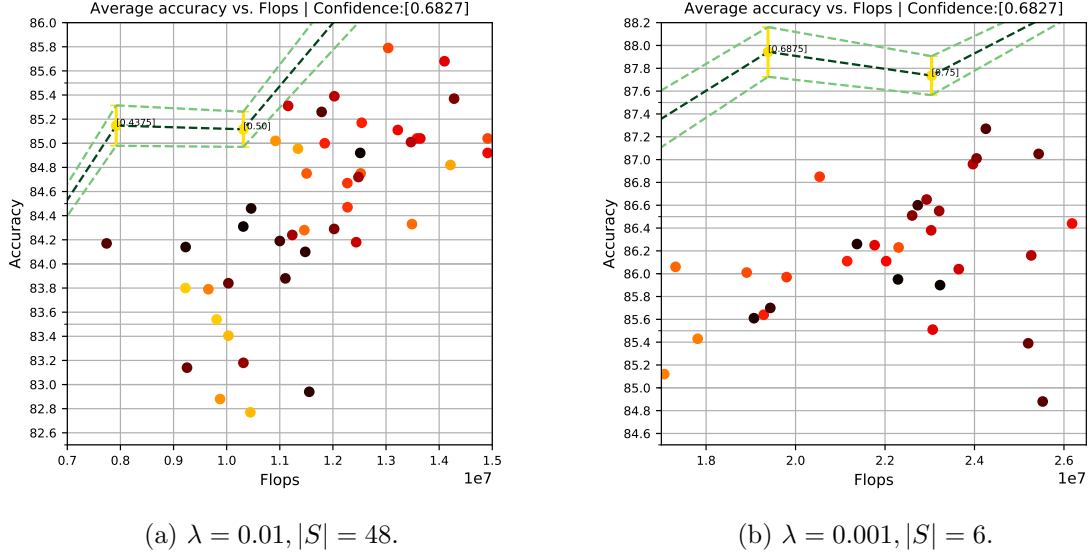
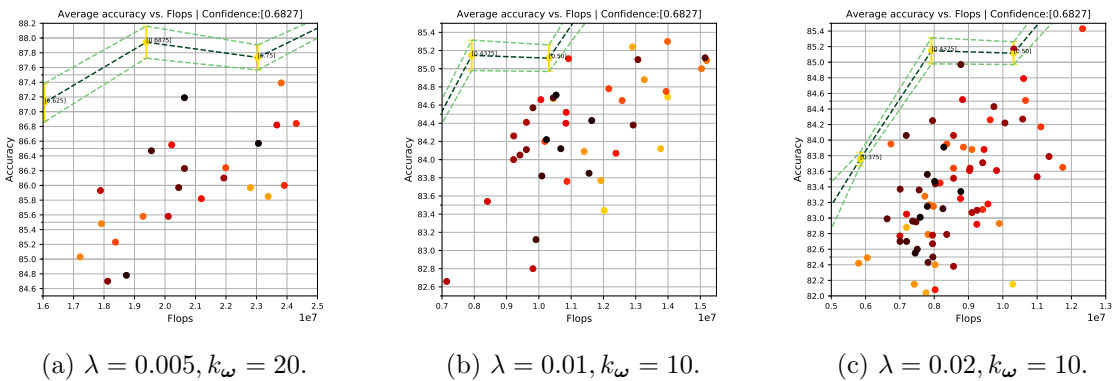


Figure B.7: Results of basic search.


 Figure B.8: Results of search with  $\omega$  resetting.  $|S| = 6$ .

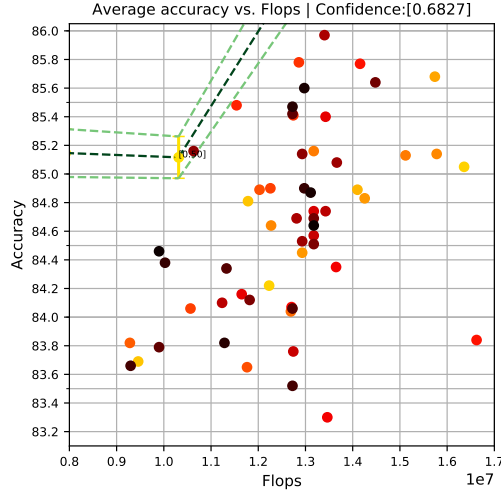
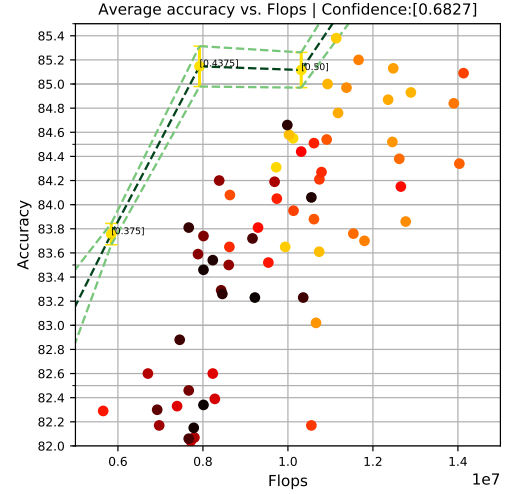

 (a)  $\lambda = 0.005, |S| = 8$ 

 (b)  $\lambda = 0.01, |S| = 6$ 

Figure B.9: Results of without weight sharing.

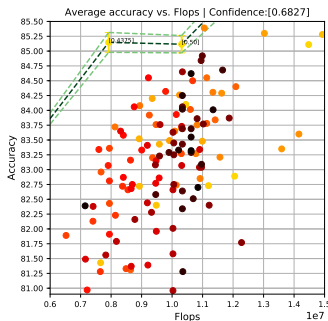
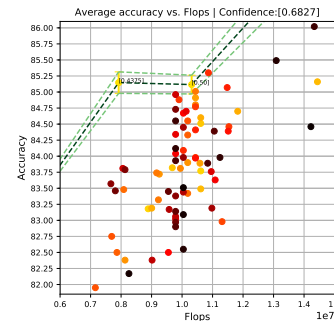
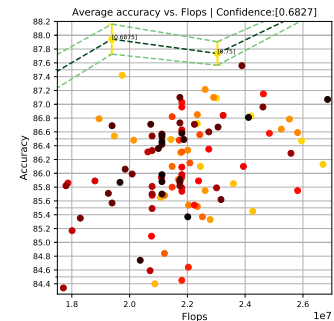

 (a) Learning rate = 5E-4. Initial distribution is 0.5, i.e.,  $\hat{\alpha}_\ell = 0.5$ .

 (b) Learning rate = 1E-4. Initial distribution is 0.5, i.e.,  $\hat{\alpha}_\ell = 0.5$ .

 (c) Learning rate = 1E-4. Initial distribution is 0.75, i.e.,  $\hat{\alpha}_\ell = 0.75$ .

Figure B.10: Results of search with interpolation loss.

## Appendix C. Search algorithms

### C.1 Quantization search algorithm

---

#### Algorithm C.1 Search method

---

```

1: Split training set  $T$  to two halves:
   •  $T_\alpha$ , a set to update distribution parameters  $\alpha$ 
   •  $T_\omega$ , a set to update network weights  $\omega$ .
2: Set bitwidth set  $T_\ell$  for each layer
3: Set an initial distribution  $\hat{\alpha}^0$ 
4: Set a configurations subset size  $|S|$  for  $J(\alpha; \omega)$  gradient estimator
5: Set  $t_\omega$ , number of epochs to train network weights in each iteration
6: Set a target homogeneous configuration  $a_{homogeneous}$  for  $\mathcal{L}_{com}(a)$ 
7: Set  $\lambda$  for  $\mathcal{L}_{com}(a)$ 
8: Set a function  $\sigma(\cdot)$  for  $\mathcal{L}_{com}(a)$ 
9: while not converged do
10:   for 1 to  $t_\omega$  do
11:     for batch  $b$  in  $T_\omega$  do
12:       Sample configuration  $a$  from current distribution  $\hat{\alpha}^k$ 
13:       Update  $\omega$  by a gradient step on  $\mathcal{L}_{acc}(a; \omega)$ 
14:     end for
15:   end for
16:   for batch  $b$  in  $T_\alpha$  do
17:     Sample configurations subset  $S_k$  from current distribution  $\hat{\alpha}^k$ 
18:     Update the distribution parameters  $\alpha$  by a gradient step on  $J(\alpha; \omega)$ 
19:   end for
20: end while
21: Sample and evaluate found configurations

```

---

## C.2 Basic pruning search method

---

**Algorithm C.2** Basic search method
 

---

```

1: Split training set  $T$  to two halves:
   •  $T_\alpha$ , a set to update distribution parameters  $\alpha$ 
   •  $T_\omega$ , a set to update network weights  $\omega$ .
2: Set an initial distribution  $\hat{\alpha}^0$ 
3: Set a homogeneous configurations set  $A$  for Slimmable method weights training
4: Set a configurations subset size,  $|S|$ , for  $J(\alpha; \omega)$  gradient estimator
5: Set  $t_\omega$ , number of epochs to train network weights in each iteration
6: Set a target homogeneous configuration  $a_{homogeneous}$  for  $\mathcal{L}_{com}(\mathbf{a})$ 
7: Set  $\lambda$  for  $\mathcal{L}_{com}(\mathbf{a})$ 
8: Set a function,  $\sigma(\cdot)$ , for  $\mathcal{L}_{com}(\mathbf{a})$ 
9: while not converged do
10:   Set Slimmable training method to train on  $A \cup \mathcal{A}^{\hat{\alpha}^k}$ 
11:   for 1 to  $t_\omega$  do
12:     for batch  $b$  in  $T_\omega$  do
13:       Update  $\omega$  by Slimmable training method gradient step
14:     end for
15:   end for
16:   for batch  $b$  in  $T_\alpha$  do
17:     Sample configurations subset  $S_k$  from current distribution  $\hat{\alpha}^k$ 
18:     Train each configuration  $\mathbf{a} \in S_k$  weights for 5 epochs over  $T_\omega$ 
19:     Update the distribution parameters  $\alpha$  by a gradient step on  $J(\alpha; \omega)$ 
20:   end for
21: end while
22: Sample and evaluate found configurations
  
```

---

### C.3 Resetting the $\omega$

---

#### Algorithm C.3 Resetting the $\omega$

---

```

1: Set training set  $T$ 
2: Set an initial distribution  $\hat{\alpha}^0$ 
3: Set a homogeneous configurations set  $A$  for Slimmable method weights training
4: Set a configurations subset size,  $|S|$ , for  $J(\boldsymbol{\alpha}; \boldsymbol{\omega})$  gradient estimator
5: Set  $t_\omega$ , number of epochs to train network weights in each iteration
6: Set  $k_\omega$ , number of iterations between  $\boldsymbol{\omega}$  update
7: Set a target homogeneous configuration  $a_{homogeneous}$  for  $\mathcal{L}_{com}(\mathbf{a})$ 
8: Set  $\lambda$  for  $\mathcal{L}_{com}(\mathbf{a})$ 
9: Set a function,  $\sigma(\cdot)$ , for  $\mathcal{L}_{com}(\mathbf{a})$ 
10: while not converged do
11:   if  $(k_\omega \bmod k) == 0$  then
12:     Set Slimmable training method to train on  $A \cup \mathcal{A}^{\hat{\alpha}^k}$ 
13:     Set random values to  $\boldsymbol{\omega}$ 
14:     for 1 to  $t_\omega$  do
15:       for batch  $b$  in  $T$  do
16:         Update  $\boldsymbol{\omega}$  by Slimmable training method gradient step
17:       end for
18:     end for
19:   end if
20:   Sample configurations subset  $S_k$  from current distribution  $\hat{\alpha}^k$ 
21:   Train each configuration  $\mathbf{a} \in S_k$  weights for 5 epochs over  $T$ 
22:   for batch  $b$  in  $T$  do
23:     Update the distribution parameters  $\alpha$  by a gradient step on  $J(\boldsymbol{\alpha}; \boldsymbol{\omega})$ 
24:   end for
25: end while
26: Sample and evaluate found configurations

```

---

In addition, we decided to make a few more changes:

- To optimize runtime, we decided to perform the training  $\boldsymbol{\omega}$ , which takes most of the time, once in 10 – 20 of updating the distribution parameters  $\alpha$ .
- We used the whole training set both for updating  $\alpha$  and  $\boldsymbol{\omega}$ .
- We decided to save more running time by evaluated the configurations in  $S_k$  on each batch in  $T$ , instead of evaluation on a single batch, which further reduced runtime.

#### C.4 Disabling weight-sharing

---

**Algorithm C.4** Disabling weight-sharing
 

---

```

1: Set training set  $T$ 
2: Set an initial distribution  $\hat{\alpha}^0$ 
3: Set a configurations subset size,  $|S|$ , for  $J(\boldsymbol{\alpha}; \boldsymbol{\omega})$  gradient estimator
4: Set  $t_{\boldsymbol{\omega}}$ , number of epochs to train a configuration weights  $\boldsymbol{\omega}_{1,2,\dots,L}$ 
5: Set a target homogeneous configuration  $a_{homogeneous}$  for  $\mathcal{L}_{com}(\boldsymbol{a})$ 
6: Set  $\lambda$  for  $\mathcal{L}_{com}(\boldsymbol{a})$ 
7: Set a function,  $\sigma(\cdot)$ , for  $\mathcal{L}_{com}(\boldsymbol{a})$ 
8: while not converged do
9:   Sample configurations subset  $S_k$  from current distribution  $\hat{\alpha}^k$ 
10:  for configuration  $\boldsymbol{a} \in S_k$  do
11:    Set random values to  $\boldsymbol{\omega}_{1,2,\dots,L}$ 
12:    for 1 to  $t_{\boldsymbol{\omega}}$  do
13:      for batch  $b$  in  $T$  do
14:        Update  $\boldsymbol{\omega}_{1,2,\dots,L}$  by a gradient step on  $\mathcal{L}_{acc}(\boldsymbol{a}; \boldsymbol{\omega}_{1,2,\dots,L})$ 
15:      end for
16:    end for
17:  end for
18:  for batch  $b$  in  $T$  do
19:    Update the distribution parameters  $\alpha$  by a gradient step on  $J(\boldsymbol{\alpha}; \boldsymbol{\omega})$ 
20:  end for
21: end while
22: Sample and evaluate found configurations
  
```

---

### C.5 Interpolation loss

---

**Algorithm C.5** Interpolation loss
 

---

```

1: Set training set  $T$ 
2: Set an initial distribution  $\hat{\alpha}^0$ 
3: Set a configurations subset size,  $|S|$ , for  $J(\boldsymbol{\alpha}; \boldsymbol{\omega})$  gradient estimator
4: Set  $t_{\boldsymbol{\omega}}$ , number of epochs to train a configuration weights  $\boldsymbol{\omega}_{1,2,\dots,L}$ 
5: Set a function,  $\sigma(\cdot)$ , for  $\mathcal{L}(\mathbf{a}; \boldsymbol{\omega})$ 
6: while not converged do
7:   Sample configurations subset  $S_k$  from current distribution  $\hat{\alpha}^k$ 
8:   for configuration  $\mathbf{a} \in S_k$  do
9:     Set random values to  $\boldsymbol{\omega}_{1,2,\dots,L}$ 
10:    for 1 to  $t_{\boldsymbol{\omega}}$  do
11:      for batch  $b$  in  $T$  do
12:        Update  $\boldsymbol{\omega}_{1,2,\dots,L}$  by a gradient step on  $\mathcal{L}_{\text{acc}}(\mathbf{a}; \boldsymbol{\omega}_{1,2,\dots,L})$ 
13:      end for
14:    end for
15:  end for
16:  for batch  $b$  in  $T$  do
17:    Update the distribution parameters  $\boldsymbol{\alpha}$  by a gradient step on  $J(\boldsymbol{\alpha}; \boldsymbol{\omega})$ 
18:  end for
19: end while
20: Sample and evaluate found configurations
  
```

---

#### C.5.1 THE EXPECTED LOSS

The expected loss is calculated by the linear interpolation between any two consecutive homogeneous configurations. For a heterogeneous configuration as  $\mathbf{a}$  with  $z_{1,2,\dots,L}$  arithmetic complexity, let  $\mathcal{L}_{\text{acc}}^{h_1, h_2}(\mathbf{a}; \boldsymbol{\omega})$  be an approximation of cross-entropy of homogeneous configuration of complexity  $a$ . Then the loss of some configuration will be:

$$\mathcal{L}(\mathbf{a}; \boldsymbol{\omega}) = \sigma \left( \mathcal{L}_{\text{acc}}(\mathbf{a}; \boldsymbol{\omega}) - \mathcal{L}_{\text{acc}}^{h_1, h_2}(\mathbf{a}; \boldsymbol{\omega}) \right) \quad (7)$$

for some increasing function  $\sigma(\cdot)$ , e.g., LeakyReLU, sigmoid or identity. Note there is no explicit arithmetic complexity loss term. For an approximation, we used a linear interpolation between two homogeneous configurations,  $a_{h_1}$  and  $a_{h_2}$ , with the closest arithmetic complexity to  $\mathbf{a}$ , such that

$$z_{h_1} \leq z_{1,2,\dots,L} \leq z_{h_2} \quad (8)$$

for a some predefined list of homogeneous configurations for which the average loss over 5 different training sessions is calculated before training.

## Appendix D. Multinomial distribution lemmas

**Lemma 1** *Let*

- Layer  $\ell$  contains  $C_\ell$  filters.
- $T_\ell$  is a set of possible operations in layer  $\ell$ .
- $\mathbf{A}_\ell$  is a random variable from a multinomial distribution, i.e.,

$$\mathbf{A}_\ell \sim \text{Multinomial}\left(C_\ell, (\hat{\alpha}_{\ell 1}, \hat{\alpha}_{\ell 2}, \dots, \hat{\alpha}_{\ell |T_\ell|})\right) \quad (9)$$

The probability to sample configuration  $a_\ell = (a_{\ell 1}, \dots, a_{\ell |T_\ell|})$  is:

$$\Pr(\mathbf{A}_\ell = a_\ell) = \frac{C_\ell!}{\prod_{k=1}^{|T_\ell|} a_{\ell k}} \cdot \frac{\exp\left\{\sum_{k=1}^{|T_\ell|} \alpha_{\ell k} \cdot a_{\ell k}\right\}}{\left(\sum_{j=1}^{|T_\ell|} \exp\{\alpha_{\ell j}\}\right)^{C_\ell}} \quad (10)$$

**Proof**

$$\begin{aligned} \Pr(\mathbf{A}_\ell = a_\ell) &= \frac{C_\ell!}{\prod_{k=1}^{|T_\ell|} a_{\ell k}} \cdot \prod_{k=1}^{|T_\ell|} (\hat{\alpha}_{\ell k})^{a_{\ell k}} \\ &= \frac{C_\ell!}{\prod_{k=1}^{|T_\ell|} a_{\ell k}} \cdot \prod_{k=1}^{|T_\ell|} \left( \frac{\exp\{\alpha_{\ell k}\}}{\sum_{j=1}^{|T_\ell|} \exp\{\alpha_{\ell j}\}} \right)^{a_{\ell k}} \\ &= \frac{C_\ell!}{\prod_{k=1}^{|T_\ell|} a_{\ell k}} \cdot \frac{\prod_{k=1}^{|T_\ell|} (\exp\{\alpha_{\ell k} \cdot a_{\ell k}\})}{\prod_{k=1}^{|T_\ell|} \left( \sum_{j=1}^{|T_\ell|} \exp\{\alpha_{\ell j}\} \right)^{a_{\ell k}}} \\ &= \frac{C_\ell!}{\prod_{k=1}^{|T_\ell|} a_{\ell k}} \cdot \frac{\exp\left\{\sum_{k=1}^{|T_\ell|} \alpha_{\ell k} \cdot a_{\ell k}\right\}}{\left(\sum_{j=1}^{|T_\ell|} \exp\{\alpha_{\ell j}\}\right)^{\sum_{k=1}^{|T_\ell|} a_{\ell k}}} \\ &= \frac{C_\ell!}{\prod_{k=1}^{|T_\ell|} a_{\ell k}} \cdot \frac{\exp\left\{\sum_{k=1}^{|T_\ell|} \alpha_{\ell k} \cdot a_{\ell k}\right\}}{\left(\sum_{j=1}^{|T_\ell|} \exp\{\alpha_{\ell j}\}\right)^{C_\ell}} \end{aligned} \quad (11)$$

■

**Lemma 2** *The partial derivative of the probability to sample layer configuration  $a_\ell$  under the multinomial distribution is:*

$$\frac{\partial}{\partial \alpha_{\ell t}} \Pr(\mathbf{A}_\ell = a_\ell) = (a_{\ell t} - C_\ell \cdot \hat{\alpha}_{\ell t}) \cdot \Pr(\mathbf{A}_\ell = a_\ell) \quad (12)$$

**Proof**

$$\begin{aligned}
\frac{\partial}{\partial \alpha_{\ell t}} \Pr(\mathbf{A}_\ell = a_\ell) &= \frac{\partial}{\partial \alpha_{\ell t}} \left( \frac{C_\ell!}{\prod_{k=1}^{|T_\ell|} a_{\ell k}} \cdot \frac{\exp \left\{ \sum_{k=1}^{|T_\ell|} \alpha_{\ell k} \cdot a_{\ell k} \right\}}{\left( \sum_{j=1}^{|T_\ell|} \exp \{ \alpha_{\ell j} \} \right)^{C_\ell}} \right) \\
&= \frac{C_\ell!}{\prod_{k=1}^{|T_\ell|} a_{\ell k}} \cdot \frac{\partial}{\partial \alpha_{\ell t}} \frac{\exp \left\{ \sum_{k=1}^{|T_\ell|} \alpha_{\ell k} \cdot a_{\ell k} \right\}}{\left( \sum_{j=1}^{|T_\ell|} \exp \{ \alpha_{\ell j} \} \right)^{C_\ell}} \\
&= \frac{C_\ell!}{\prod_{k=1}^{|T_\ell|} a_{\ell k}} \cdot \frac{1}{\left( \sum_{j=1}^{|T_\ell|} \exp \{ \alpha_{\ell j} \} \right)^{C_\ell} \cdot \left( \sum_{j=1}^{|T_\ell|} \exp \{ \alpha_{\ell j} \} \right)^{C_\ell}} \\
&\quad \left[ \left( \sum_{j=1}^{|T_\ell|} \exp \{ \alpha_{\ell j} \} \right)^{C_\ell} \cdot \frac{\partial}{\partial \alpha_{\ell t}} \exp \left\{ \sum_{k=1}^{|T_\ell|} \alpha_{\ell k} \cdot a_{\ell k} \right\} - \right. \\
&\quad \left. - \exp \left\{ \sum_{k=1}^{|T_\ell|} \alpha_{\ell k} \cdot a_{\ell k} \right\} \cdot \frac{\partial}{\partial \alpha_{\ell t}} \left( \sum_{j=1}^{|T_\ell|} \exp \{ \alpha_{\ell j} \} \right)^{C_\ell} \right] \tag{13} \\
&= \frac{C_\ell!}{\prod_{k=1}^{|T_\ell|} a_{\ell k}} \cdot \left( a_{\ell t} \cdot \frac{\exp \left\{ \sum_{k=1}^{|T_\ell|} \alpha_{\ell k} \cdot a_{\ell k} \right\}}{\left( \sum_{j=1}^{|T_\ell|} \exp \{ \alpha_{\ell j} \} \right)^{C_\ell}} - \right. \\
&\quad \left. - C_\ell \cdot \frac{\exp \{ a_{\ell t} \}}{\sum_{j=1}^{|T_\ell|} \exp \{ \alpha_{\ell j} \}} \cdot \frac{\exp \left\{ \sum_{k=1}^{|T_\ell|} \alpha_{\ell k} \cdot a_{\ell k} \right\}}{\left( \sum_{j=1}^{|T_\ell|} \exp \{ \alpha_{\ell j} \} \right)^{C_\ell}} \right) \\
&= a_{\ell t} \cdot \Pr(\mathbf{A}_\ell = a_\ell) - C_\ell \cdot \hat{\alpha}_{\ell t} \cdot \Pr(\mathbf{A}_\ell = a_\ell) \\
&= (a_{\ell t} - C_\ell \cdot \hat{\alpha}_{\ell t}) \cdot \Pr(\mathbf{A}_\ell = a_\ell)
\end{aligned}$$

■

**Lemma 3** *The partial derivative of the probability  $p(\mathbf{a}|\boldsymbol{\alpha})$  to sample network configuration  $\mathbf{a}$  under the multinomial distribution is:*

$$\frac{\partial}{\partial \alpha_{\ell t}} p(\mathbf{a}|\boldsymbol{\alpha}) = (a_{\ell t} - C_\ell \cdot \hat{\alpha}_{\ell t}) \cdot p(\mathbf{a}|\boldsymbol{\alpha}) \tag{14}$$

**Proof**

$$\begin{aligned}
\frac{\partial}{\partial \alpha_{\ell t}} p(\mathbf{a}|\boldsymbol{\alpha}) &= \frac{\partial}{\partial \alpha_{\ell t}} \prod_{r=1}^L \Pr(\mathbf{A}_r = a_r) \\
&= \prod_{r \neq \ell} \Pr(\mathbf{A}_r = a_r) \cdot \frac{\partial}{\partial \alpha_{\ell t}} \Pr(\mathbf{A}_\ell = a_\ell) \\
&= \prod_{r \neq \ell} \Pr(\mathbf{A}_r = a_r) \cdot ((a_{\ell t} - C_\ell \cdot \hat{\alpha}_{\ell t}) \cdot \Pr(\mathbf{A}_\ell = a_\ell)) \quad (15) \\
&= (a_{\ell t} - C_\ell \cdot \hat{\alpha}_{\ell t}) \prod_{r=1}^L \Pr(\mathbf{A}_r = a_r) \\
&= (a_{\ell t} - C_\ell \cdot \hat{\alpha}_{\ell t}) \cdot p(\mathbf{a}|\boldsymbol{\alpha})
\end{aligned}$$

■

**Lemma 4** *The partial derivative of the loss expected value  $J(\boldsymbol{\alpha}; \boldsymbol{\omega})$  under the multinomial distribution is:*

$$\frac{\partial}{\partial \alpha_{\ell t}} J(\boldsymbol{\alpha}; \boldsymbol{\omega}) = \sum_{\mathbf{a}} \mathcal{L}(\mathbf{a}; \boldsymbol{\omega}) \cdot (a_{\ell t} - C_\ell \cdot \hat{\alpha}_{\ell t}) \cdot p(\mathbf{a}|\boldsymbol{\alpha}) \quad (16)$$

**Proof**

$$\begin{aligned}
\frac{\partial}{\partial \alpha_{\ell t}} J(\boldsymbol{\alpha}; \boldsymbol{\omega}) &= \frac{\partial}{\partial \alpha_{\ell t}} \sum_{\mathbf{a}} p(\mathbf{a}|\boldsymbol{\alpha}) \cdot \mathcal{L}(\mathbf{a}; \boldsymbol{\omega}) \\
&= \sum_{\mathbf{a}} \mathcal{L}(\mathbf{a}; \boldsymbol{\omega}) \cdot \frac{\partial}{\partial \alpha_{\ell t}} p(\mathbf{a}|\boldsymbol{\alpha}) \quad (17) \\
&= \sum_{\mathbf{a}} \mathcal{L}(\mathbf{a}; \boldsymbol{\omega}) \cdot (a_{\ell t} - C_\ell \cdot \hat{\alpha}_{\ell t}) \cdot p(\mathbf{a}|\boldsymbol{\alpha})
\end{aligned}$$

■

where  $a_{\ell t}$  represents on how many filters in layer  $\ell$  in configuration  $\mathbf{a}$  we apply operation  $t$ .

**Appendix E. Binomial distribution lemmas**

**Lemma 5** *Let*

- Layer  $\ell$  contains  $C_\ell$  filters.

- $\mathbf{A}_\ell$  is a random variable from a binomial distribution, i.e.,

$$\mathbf{A}_\ell \sim \text{Binomial}(C_\ell - 1, \hat{\alpha}_\ell) \quad (18)$$

The probability to sample configuration  $a_\ell = (a_\ell)$  is:

$$\Pr(\mathbf{A}_\ell = a_\ell) = \frac{(C_\ell - 1)!}{a_\ell! \cdot (C_\ell - 1 - a_\ell)!} \cdot \frac{\exp\{\alpha_\ell \cdot a_\ell\}}{(\exp\{\alpha_\ell\} + 1)^{(C_\ell - 1)}} \quad (19)$$

## Proof

$$\begin{aligned} \Pr(\mathbf{A}_\ell = a_\ell) &= \binom{C_\ell - 1}{a_\ell} \cdot (\hat{\alpha}_\ell)^{a_\ell} \cdot (1 - \hat{\alpha}_\ell)^{(C_\ell - 1) - a_\ell} \\ &= \frac{(C_\ell - 1)!}{a_\ell! \cdot (C_\ell - 1 - a_\ell)!} \cdot \left( \frac{\exp\{\alpha_\ell\}}{\exp\{\alpha_\ell\} + 1} \right)^{a_\ell} \cdot \left( 1 - \frac{\exp\{\alpha_\ell\}}{\exp\{\alpha_\ell\} + 1} \right)^{(C_\ell - 1) - a_\ell} \\ &= \frac{(C_\ell - 1)!}{a_\ell! \cdot (C_\ell - 1 - a_\ell)!} \cdot \left( \frac{\exp\{\alpha_\ell\}}{\exp\{\alpha_\ell\} + 1} \right)^{a_\ell} \cdot \left( \frac{1}{\exp\{\alpha_\ell\} + 1} \right)^{(C_\ell - 1) - a_\ell} \\ &= \frac{(C_\ell - 1)!}{a_\ell! \cdot (C_\ell - 1 - a_\ell)!} \cdot \frac{\exp\{\alpha_\ell \cdot a_\ell\}}{(\exp\{\alpha_\ell\} + 1)^{(C_\ell - 1)}} \end{aligned} \quad (20)$$

■

**Lemma 6** The partial derivative of the probability to sample layer configuration  $a_\ell$  under the binomial distribution is:

$$\frac{\partial}{\partial \alpha_\ell} \Pr(\mathbf{A}_\ell = a_\ell) = (a_\ell - (C_\ell - 1) \cdot \hat{\alpha}_\ell) \cdot \Pr(\mathbf{A}_\ell = a_\ell) \quad (21)$$

## Proof

$$\begin{aligned}
\frac{\partial}{\partial \alpha_\ell} \Pr(\mathbf{A}_\ell = a_\ell) &= \frac{\partial}{\partial \alpha_\ell} \left( \frac{(C_\ell - 1)!}{a_\ell! \cdot (C_\ell - 1 - a_\ell)!} \cdot \frac{\exp \{\alpha_\ell \cdot a_\ell\}}{(\exp \{\alpha_\ell\} + 1)^{(C_\ell - 1)}} \right) \\
&= \frac{(C_\ell - 1)!}{a_\ell! \cdot (C_\ell - 1 - a_\ell)!} \cdot \frac{\partial}{\partial \alpha_\ell} \frac{\exp \{\alpha_\ell \cdot a_\ell\}}{(\exp \{\alpha_\ell\} + 1)^{(C_\ell - 1)}} \\
&= \frac{(C_\ell - 1)!}{a_\ell! \cdot (C_\ell - 1 - a_\ell)!} \cdot \frac{1}{(\exp \{\alpha_\ell\} + 1)^{(C_\ell - 1)} \cdot (\exp \{\alpha_\ell\} + 1)^{(C_\ell - 1)}} \\
&\quad \left( (\exp \{\alpha_\ell\} + 1)^{(C_\ell - 1)} \cdot \frac{\partial}{\partial \alpha_\ell} \exp \{\alpha_\ell \cdot a_\ell\} \right. \\
&\quad \left. - \exp \{\alpha_\ell \cdot a_\ell\} \cdot \frac{\partial}{\partial \alpha_\ell} (\exp \{\alpha_\ell\} + 1)^{(C_\ell - 1)} \right) \tag{22} \\
&= \frac{(C_\ell - 1)!}{a_\ell! \cdot (C_\ell - 1 - a_\ell)!} \cdot \left( \frac{a_\ell \cdot \exp \{\alpha_\ell \cdot a_\ell\}}{(\exp \{\alpha_\ell\} + 1)^{(C_\ell - 1)}} \right. \\
&\quad \left. - (C_\ell - 1) \cdot \frac{\exp \{\alpha_\ell \cdot a_\ell\}}{(\exp \{\alpha_\ell\} + 1)^{(C_\ell - 1)}} \cdot \frac{\exp \{\alpha_\ell\}}{\exp \{\alpha_\ell\} + 1} \right) \\
&= \frac{(C_\ell - 1)!}{a_\ell! \cdot (C_\ell - 1 - a_\ell)!} \cdot \frac{\exp \{\alpha_\ell \cdot a_\ell\}}{(\exp \{\alpha_\ell\} + 1)^{(C_\ell - 1)}} \cdot (a_\ell - (C_\ell - 1) \cdot \hat{\alpha}_\ell) \\
&= (a_\ell - (C_\ell - 1) \cdot \hat{\alpha}_\ell) \cdot \Pr(\mathbf{A}_\ell = a_\ell)
\end{aligned}$$

■

**Lemma 7** *The partial derivative of the probability  $p(\mathbf{a}|\boldsymbol{\alpha})$  to sample network configuration  $\mathbf{a}$  under the binomial distribution is:*

$$\frac{\partial}{\partial \alpha_{\ell t}} p(\mathbf{a}|\boldsymbol{\alpha}) = (a_\ell - (C_\ell - 1) \cdot \hat{\alpha}_\ell) \cdot p(\mathbf{a}|\boldsymbol{\alpha}) \tag{23}$$

**Proof**

$$\begin{aligned}
 \frac{\partial}{\partial \alpha_\ell} p(\mathbf{a}|\boldsymbol{\alpha}) &= \frac{\partial}{\partial \alpha_\ell} \prod_{r=1}^L \Pr(\mathbf{A}_r = a_r) \\
 &= \prod_{r \neq \ell} \Pr(\mathbf{A}_r = a_r) \cdot \frac{\partial}{\partial \alpha_\ell} \Pr(\mathbf{A}_\ell = a_\ell) \\
 &= \prod_{r \neq \ell} \Pr(\mathbf{A}_r = a_r) \cdot ((a_\ell - (C_\ell - 1) \cdot \hat{\alpha}_\ell) \cdot \Pr(\mathbf{A}_\ell = a_\ell)) \\
 &= (a_\ell - (C_\ell - 1) \cdot \hat{\alpha}_\ell) \cdot \prod_{r=1}^L \Pr(\mathbf{A}_r = a_r) \\
 &= (a_\ell - (C_\ell - 1) \cdot \hat{\alpha}_\ell) \cdot p(\mathbf{a}|\boldsymbol{\alpha})
 \end{aligned} \tag{24}$$

■

**Lemma 8** *The partial derivative of the loss expected value  $J(\boldsymbol{\alpha}; \boldsymbol{\omega})$  under the binomial distribution is:*

$$\frac{\partial}{\partial \alpha_\ell} J(\boldsymbol{\alpha}; \boldsymbol{\omega}) = \sum_{\mathbf{a}} \mathcal{L}(\mathbf{a}; \boldsymbol{\omega}) \cdot (a_\ell - (C_\ell - 1) \cdot \hat{\alpha}_\ell) \cdot p(\mathbf{a}|\boldsymbol{\alpha}) \tag{25}$$

**Proof**

$$\begin{aligned}
 \frac{\partial}{\partial \alpha_\ell} J(\boldsymbol{\alpha}; \boldsymbol{\omega}) &= \frac{\partial}{\partial \alpha_\ell} \sum_{\mathbf{a}} p(\mathbf{a}|\boldsymbol{\alpha}) \cdot \mathcal{L}(\mathbf{a}; \boldsymbol{\omega}) \\
 &= \sum_{\mathbf{a}} \mathcal{L}(\mathbf{a}; \boldsymbol{\omega}) \cdot \frac{\partial}{\partial \alpha_\ell} p(\mathbf{a}|\boldsymbol{\alpha}) \\
 &= \sum_{\mathbf{a}} \mathcal{L}(\mathbf{a}; \boldsymbol{\omega}) \cdot (a_\ell - (C_\ell - 1) \cdot \hat{\alpha}_\ell) \cdot p(\mathbf{a}|\boldsymbol{\alpha})
 \end{aligned} \tag{26}$$

■

where  $a_\ell$  represents on how many filters in layer  $\ell$  in configuration  $\mathbf{a}$  we apply the operation.

## Appendix F. BOPs definition and loss derivation

Under quantization as a constraint, we use BOPs as arithmetic complexity metric. The BOPs metric quantifying the number of bit operations. Given the bitwidth of two operands,

it is possible to approximate the number of bit operations required for a basic arithmetic operation such as addition and multiplication.

An important phenomenon is the non-linear relation between the number of activation and weight bits and the resulting network complexity in BOPs. To quantify this effect, let us consider a single convolutional layer with  $b_w$ -bit weights and  $b_a$ -bit activations containing  $n$  input channels,  $m$  output channels, and  $k \times k$  filters. The maximum value of a single output is about  $2^{b_a+b_w} nk^2$ , which sets the accumulator width in the MAC operations to  $b_o = b_a + b_w + \log_2 nk^2$ . The complexity of a single output calculation consists therefore of  $nk^2 b_a$ -wide  $\times b_w$ -wide multiplications and about the same amount of  $b_o$ -wide additions. This yields the total layer complexity of

$$\text{BOPs} \approx mnk^2(b_a b_w + b_a + b_w + \log_2 nk^2). \quad (27)$$

Note that the reduction of the weight and activation bitwidth decreases the number of BOPs as long as the factor  $b_a b_w$  dominates the factor  $\log_2 nk^2$ . Since the latter factor depends only on the layer topology, this point of diminishing return is network architecture-dependent. Another factor that must be incorporated into the BOPs calculation is the cost of fetching the parameters from an external memory. Two assumptions are made in the approximation of this cost: firstly, we assume that each parameter is only fetched once from an external memory; secondly, the cost of fetching a  $b$ -bit parameter is assumed to be  $b$  BOPs. Given a neural network with  $n$  parameters all represented in  $b$  bits, the memory access cost is simply  $nb$ .

## F.1 BOPs loss derivation

Since custom precision data types are used for the network weights and activations, the number of MAC operations (Kahan, 1996) is not an appropriate metric to accurately estimate the computational complexity of the desired model. Recently, Baskin *et al.* (Baskin et al., 2018b) proposed *Bit Operations (BOPs)* as a metric to quantify the computational complexity of neural networks with multiple bitwidths. However, since we need to take into account filter-wise granularity, the exact expression for BOPs is slightly different.

Nevertheless, the main idea is the same. We denote by  $b_t^\omega$  and  $b_t^\alpha$  bitwidth of weights and activations for operation type  $t$ . For a filter in the  $n$ -th convolutional layer, the filter's output is of shape  $c_n \times H \times W$ . For simplicity we assume the filter is a  $k_n \times k_n$  square.

The operation of convolution can be viewed as alternating multiplications of the input pixel by the weight and addition of the result to the accumulator, which stores the result of the convolution. While the cost of multiplication is obviously  $b_{t_1}^\alpha b_{t_2}^\omega$ , the cost of addition is a bit harder to approximate.

The accumulator needs to be able to store any possible result of the convolution, and thus approximate the required bitwidth with maximal value of a single filter of bitwidth  $b_{t_2}^\omega$ ,

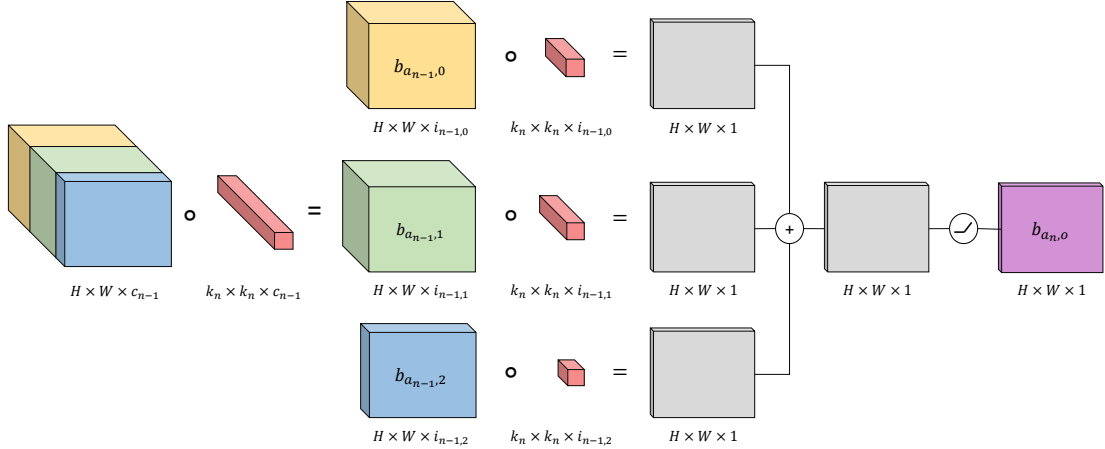


Figure F.1: Applying a  $(b_{\omega_n,o}, b_{a_n,o})$  filter of the  $n$ -th layer, *i.e.*, the filter weights are quantized using  $b_{\omega_n,o}$  bits and its activation (output) uses  $b_{a_n,o}$  bits.

which is a sum of maximal values of each multiplication

$$M_{n,t_2} = \sum_{t_1 \in T} a_{n-1,t_1} 2^{b_{t_2}^\omega + b_{t_1}^a} k_n^2 = 2^{b_{t_2}^\omega} k_n^2 \sum_{t_1=1}^m a_{n-1,t_1} 2^{b_{t_1}^a}, \quad (28)$$

which sets the accumulator width to

$$b_{n,t_2}^{\text{AW}} = \log_2 M_{n,t_2} \approx b_{t_2}^\omega \log_2 \sum_{t_1 \in T} a_{n-1,t_1} 2^{b_{t_1}^\alpha}. \quad (29)$$

Therefore, the complexity of computing the single pixel of a single filter is

$$\mathcal{B}_{n,t_2}(\mathbf{a}) = k_n^2 \left[ c_{n-1} b_{n,t_2}^{\text{AW}} + \sum_{t_1 \in T} a_{n-1,t_1} b_{t_1}^\alpha b_{t_2}^\omega \right] \quad (30)$$

This yields the total layer complexity of

$$\mathcal{B}_n(\mathbf{a}) \approx HW \sum_{t_1 \in T} \mathcal{B}_{n,t_2}(\mathbf{a}) \quad (31)$$

The proposed metric is useful when the inference is performed on a custom hardware like FPGAs or ASICs. Both are natural choices for quantized networks, due to the use of lookup tables (LUTs) and dedicated MAC (or more general DSP) units, which are efficient with custom data types.